

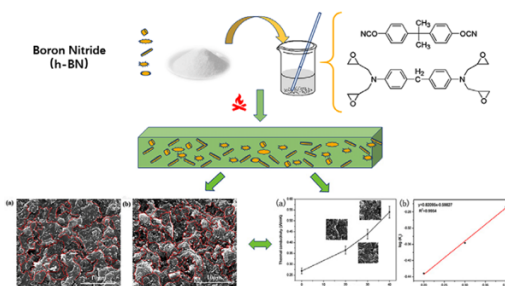
# Design of h-BN-Filled Cyanate/Epoxy Thermal Conductive Composite with Stable Dielectric Properties

Yangxue Lei  
Zengmao Han  
Dengxun Ren  
Hai Pan  
Mingzhen Xu\*  
Xiaobo Liu\*

Research Branch of Advanced Functional Materials, School of Materials and Energy,  
University of Electronic Science and Technology of China, Chengdu, 611731, P. R. China

Received September 15, 2017 / Revised January 2, 2018 / Accepted February 9, 2018

**Abstract:** The thermal conductive cyanate ester/epoxy (CE/AG80) composites with hexagonal boron nitride (h-BN) reinforced were manufactured and investigated. The low and stable dielectric constant/loss of the composites with respect to both frequency (500 Hz–100 kHz) and temperature (50–350 °C) were discussed as functions of the content of h-BN. It was found that the low and stable dielectric constant/loss of the composites can be maintained in the whole frequency range at room temperature, and the mutations of constant/loss at the frequency of 1 kHz occurred above 280 °C for all of the samples. Moreover, a remarkable enhancement of the thermal conductivity (0.54 W/mK a 1.8-fold enhancement) was achieved with the introduction of h-BN and significantly outperformed traditional thermal conductive fillers. The significant improvements of the thermal conductivity of the composites were analyzed by the Agari's model and the parameters of  $C_1$  and  $C_2$  were also calculated.



**Keywords:** dielectric properties, thermal conductivity, composites, hexagonal boron nitride.

## 1. Introduction

With the miniaturization and densification of the electronic components, increasingly high requires for the substrate materials including high frequency stability, high reliability and low power consumption have been put forward.<sup>1,2</sup> Moreover, good thermal conductivity is also one of the key characters for the novel electric materials.<sup>3</sup> In the regard of good thermal conductivity, the inherent adiabaticity and insulativity of traditional polymers for instance polymers could not meet the requirements for practical applications. In order to improve the conductive properties, various thermal conductive fillers, such as AlN, SiC, Al<sub>2</sub>O<sub>3</sub>, have been filled into the polymer matrices.<sup>4–6</sup> Nevertheless, the above fillers possess relatively high dielectric constants. Moreover, high dielectric constants would result to high power loss, which put them at a serious disadvantage when used for the electronic insulation materials. Specially, BN fillers are one of the potential conductive fillers which exhibits extremely high thermal conductivity ( $\geq 280$  W/mK).<sup>4</sup> Also, the low dielectric constants, marked chemical inertness and excellent mechanical properties, enable them candidates of the composites for electric insulation applications.

Moreover, many researchers have done related studies to

improve the thermal conductive properties, including the choices of different polymers, various dispersion methods and so on. For example, Zhou *et al.* prepared a novel fiber-reinforced polyethylene composite with Si<sub>3</sub>N<sub>4</sub> fillers *via* a conventional method of hot molding.<sup>7</sup> Kimiyasu Sato *et al.* investigated a thermally conductive composite film with the polyimide as plastic matrix and h-BN particles as fillers.<sup>8</sup> Also, Yu *et al.* prepared the polystyrene/AlN polymer composites and they achieved a special dispersion state in the composites, in which AlN particles were surrounded by the polystyrene matrix particles.<sup>9</sup> Moreover, Kemaloglu *et al.* prepared the thermally conductive BN/styrene-ethylene-butylene-styrene terpolymer/poly(ethylene-co-vinyl acetate) ternary composites and Huang *et al.* studied the electrical and thermophysical properties of ethylene-vinyl acetate elastomer composites with surface modified BaTiO<sub>3</sub> fillers.<sup>10,11</sup> In sum, various kinds of thermal conductivity nanoparticles have been used to prepare the resin matrices composites. However, compared with other polymers, epoxy/cyanate polymers have been widely used, such as electronic packaging, defense industry, aerospace fields and so on, because of their superior electrical resistivity, excellent mechanical properties and chemical stability. Meanwhile, the cost of epoxy/cyanate polymer is low which would also broaden the scope of their applications.

In this work, hexagonal boron nitride (h-BN) fillers were filled in the cyanate ester/epoxy (CE/AG80) matrices by melting mixing at a high speed. As consequence, a composite with low and stable dielectric properties and high thermal conductivity could be achieved. Meanwhile, the effects of the h-BN filler content on the microstructure, dielectric properties with respect

**Acknowledgments:** The authors wish to thank for financial support from the National Natural Science Foundation (No. 51373028, No. 51403029), and South Wisdom Valley Innovative Research Team Program.

\*Corresponding Authors: Mingzhen Xu (mzxu628@uestc.edu.cn), Xiaobo Liu (liuxb@uestc.edu.cn)

both to frequency and temperature were also discussed in detail.

## 2. Experimental

### 2.1. Raw materials

The 4,4'-(propane-2, 2-diyl)bis(cyanatobenzene) (CE), AG80 (EWW=117-134 g/mol), Imidazole and h-BN powders were commercially available and used as received without further purification.

### 2.2. Preparation of CE/AG80/h-BN composites

The detailed procedure for the preparation of CE/AG80/h-BN composites was as following. The required amount of epoxy resin and cyanate with a ratio of 4 to 6 were melted and mixed at 100 °C with imidazole added. Then, h-BN was added, containing stirring for another 3 h. The h-BN proportion was 0 wt%-40 wt%. The mixtures of CE/AG80/h-BN were poured into the preheated molds at 100 °C and cured with standard procedure. The detailed temperatures and times of curing procedures of AG80/CE/h-BN copolymers are as follows: 120 °C for 2 h, 160 °C for 2 h, 200 °C for 2 h, 220 °C for 2 h, and 250 °C for 2 h.

### 2.3. Characterizations

Scanning electron microscope (SEM, JSM25900LV) was employed to observe the morphology of the fractured surfaces of the polymers. Fourier transform infrared (FTIR) spectra were recorded by utilizing Shimadzu FTIR8400S (Japan) spectrometer in KBr pellets between 3000 and 500  $\text{cm}^{-1}$  in air. Dielectric properties of the CE/AG80/h-BN polymers were tested by a TH 2819A precision LCR meter (Tong hui Electronic Co., Ltd.), which was carried out at different frequencies (500 Hz-100 kHz) at room temperature with 40 % humidity, and at various temperatures (50-350 °C) at the frequency of 1 kHz. Dynamic mechanical analysis (DMA) in a three-point-blending mode was performed on QDMA-800 dynamic mechanical analyzer (TA Instruments, USA) to determine the glass temperature ( $T_g$ ). The tan delta were studied with the amplitude of 15  $\mu\text{m}$  and a frequency of 1 Hz, and the composites were all heated from

50 °C to 350 °C at a temperature ramp of 3 °C/min. TGA was performed on a TA Instruments TGA Q50 with a heating rate of 20 °C/min (under nitrogen or air) and a purge flow rate of 40 mL/min. Thermal conductivity measured with Netzsch LFA 457 Laser Flash Apparatus.

## 3. Results and discussion

### 3.1. Thermal conductivity of the CE/AG80/h-BN composites

As expected, the thermal conductivities of the CE/AG80/h-BN composites are strongly dependent on the content of h-BN, with higher contents consistently resulting to higher thermal conductivity, shown in Figure 1(a). When the h-BN content is 40 wt%, the thermal conductivity of the CE/AG80 composite achieves 0.54 W/mK a 1.8-fold improvement, which shows large advantages comparing with that of epoxy composites filled with AlN,  $\text{Si}_3\text{N}_4$  and copper particles.<sup>1,3,12,13</sup>

In h-BN, the inside BN layers functions as highly conductive channels for thermal transport, while the heat treated outside layers would afford sufficient covalent and non-covalent bonding with the matrix molecule chains, and facilitates the phonon transfer from the h-BN to the polymer matrices.<sup>14</sup> The semi-empirical model (Agari's model) based on the generalization of series and parallel conduction models in composites and correlates thermal conductivity with the ability of fillers to create particle conductive chains is:<sup>15</sup>

$$\log K_c = \varphi C_2 \log K_f + (1 - \varphi) \log C_1 K_p$$

where  $K_c$ ,  $K_f$  and  $K_p$  are corresponding to the thermal conductivity of the composites, the fillers and the polymer matrices, respectively.  $\varphi$  is the filler volume/weight fraction,  $C_1$  and  $C_2$  are obtained by fitting the experimental data. The logarithmic plot of thermal conductivity with respect to the filler content is presented in Figure 1(b), and the two parameters  $C_1$  and  $C_2$  are calculated to be 0.934 and 0.1593. The value of  $C_1$  suggests the introduction of h-BN would affect the curing process of the polymer chains and decreases the crosslinking degree of the matrices. The low value of  $C_2$  suggests that the h-BN in this work is hard to create thermal conductive channels efficiently under the conditions. While, considering of the increased thermal

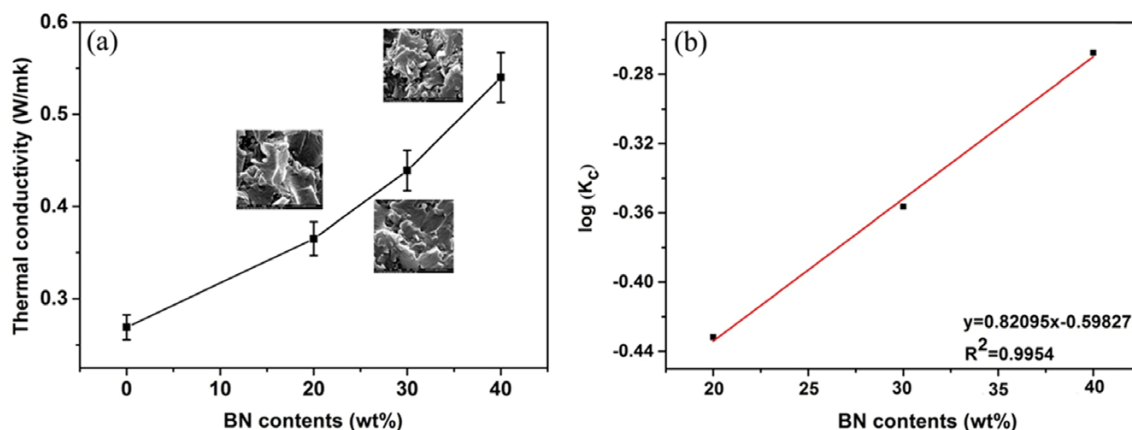


Figure 1. Thermal conductivity of CE/AG80 composites with various contents of h-BN fillers.

conductivity, it can be concluded that although it's hard, the effective conductive channels have been formed with increasing the content of h-BN. Thus, for the AG80/CE/h-BN polymers, the main heat transfer mechanism is heat conduction, *via* the phonon. After adding the h-BN fillers, many BN particles could touch each other and begin to form the thermal conductive pathways. Finally, these pathways would form the network to improve the thermal conductive of AG80/CE polymers.

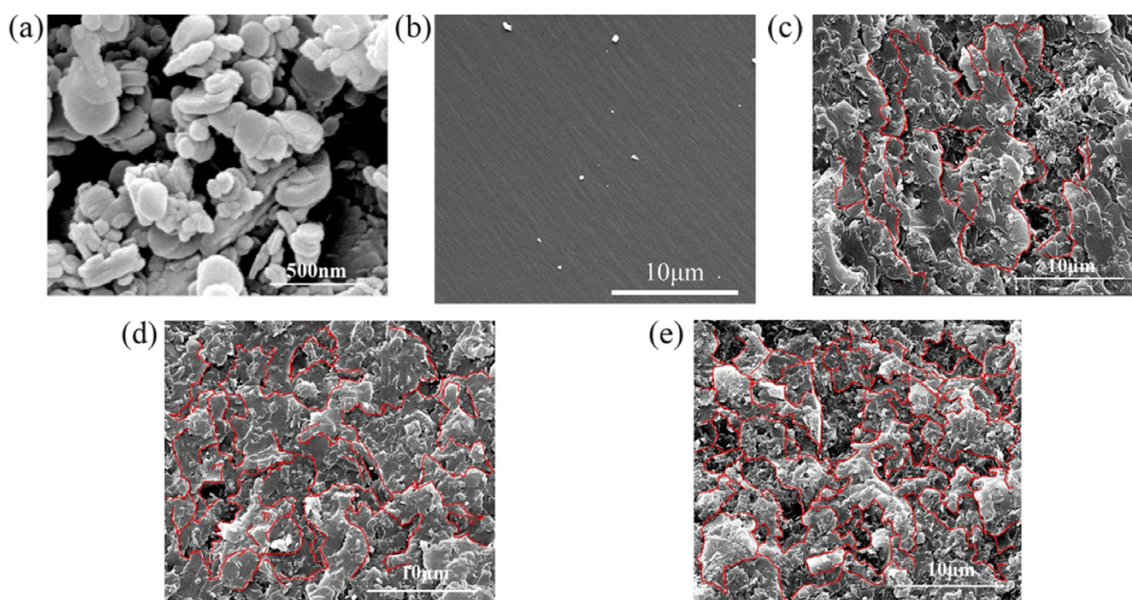
### 3.2. Morphological properties

Figure 2 shows the SEM images of the h-BN and the h-BN filled CE/AG80 composites to investigate the fracture morphology of samples. It can be seen obviously that the pure h-BN is suborbiculate with uniform size of ~100 nm diameter (Figure 2(a)). Figure 2(b)-(d) presents the fracture surface of CE/AG80 composites with various contents of h-BN fillers. It can be seen that the suborbiculate h-BN is well embedded in the CE/AG80 matrix-

ces. No aggregation and bare h-BN can be observed in the fracture surface, indicating the good dispersion and excellent interface compatibility of h-BN in the matrices. Moreover, the composites with low content of h-BN exhibit obvious resin-rich regions that without conductive fillers existence (Figure 1(b)), and the h-BN is seldom mutual contact and overlap each other, hard to form an effective conductive channel (shown in Figure 1(b)), resulting to a slighter improvement for the thermal conductivity. With increasing the content of h-BN, the contact and overlap will increase significantly and be conducive to the formation of conductive channels, contributing to the significantly improvement of conductivity (shown in Figure 1(c) and (d)).

### 3.3. Structure characterization of the h-BN and their composites

FTIR were used to investigate the introduction of h-BN and the structure transition of the CE/AG80 resin matrix after being



**Figure 2.** SEM images of CE/AG80/h-BN composites with various contents of h-BN: (a) neat h-BN, (b) without BN (c) with 20 wt% h-BN, (d) with 30 wt% h-BN and (e) with 40 wt% h-BN 10 μm.

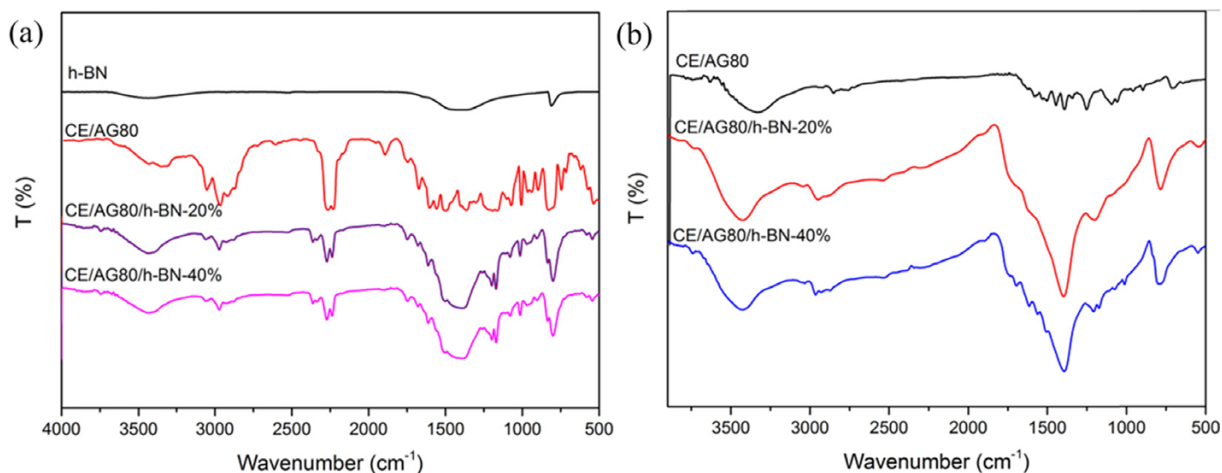


**Figure 3.** FTIR spectra of h-BN and their composites (a) pre-heated at 100 °C and (b) cured at 250 °C.

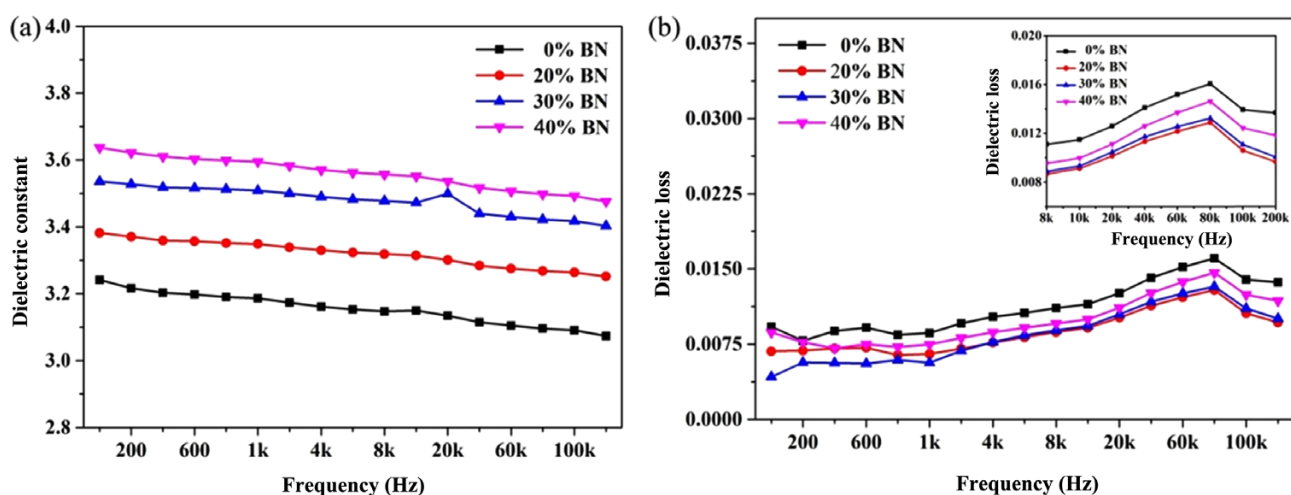


**Figure 4.** Dielectric properties with respect to frequency of CE/AG80 composites with various contents of h-BN: (a) Dielectric constant and (b) dielectric loss.

heat treated at various conditions.<sup>16</sup> Figure 3(a) and (b) presented the structures of the CE/AG80/h-BN composites treated at 100 °C and 250 °C, respectively. In Figure 3(a), the spectra of pristine h-BN and CE/AG80 without h-BN were shown, in order to make a clear comparison with that of the composites with h-BN. It can be seen that the absorption peaks near 1289 and 803  $\text{cm}^{-1}$  assigning to the B-N are observed for the pristine h-BN, and the corresponding peaks can be observed in the composites of CE/AG80/h-BN-20% and CE/AG80/h-BN-40%, indicating the incorporation of h-BN and the resin matrix. Moreover, the characteristics of the CE (C-N, 2236/2270  $\text{cm}^{-1}$ ) and AG80 (913/917  $\text{cm}^{-1}$ ) can be also observed in Figure 3(a). After being heat treated at 250 °C, the characteristics absorption peaks of the composites are shown in Figure 3(b). The absorption peaks of B-N can be observed in the composites of CE/AG80/h-BN-20% and CE/AG80/h-BN-40%, shown in Figure 3(b). Additionally, the epoxide groups (913/917  $\text{cm}^{-1}$ ) and cyanate groups (2236/2270  $\text{cm}^{-1}$ ) disappear after being treated at elevated temperature. The triazine structures (the characteristic bands are 1348  $\text{cm}^{-1}$  and 1565  $\text{cm}^{-1}$ ) can be observed which are generated by the self-polymerization of cyanate resins. Also, the oxazolidione structure (1750  $\text{cm}^{-1}$ ) appears in Figure 3(b), indicating the copolymerization of CE and AG80. Thus, the structures of the CE/AG80/h-BN composites can be confirmed with the FTIR spectra, demonstrating the incorporation of h-BN and the copolymerization of CE and AG80.

### 3.4. Dielectric properties of the CE/AG80/h-BN composites

The variations of dielectric constant and loss with respect to frequency for the CE/AG80 composites with various contents of h-BN fillers are shown in Figure 4. It's well known that the dielectric properties for the nano-composites are determined by the dielectric polarization and the relaxation mechanisms in the bulk of the composites.<sup>2</sup> In this case, polarizations associated with the polymer matrices and h-BN fillers as well as the interface polarizations occur at the matrix-filler interface would coexist. It can be seen in Figure 4(a) that the dielectric constant

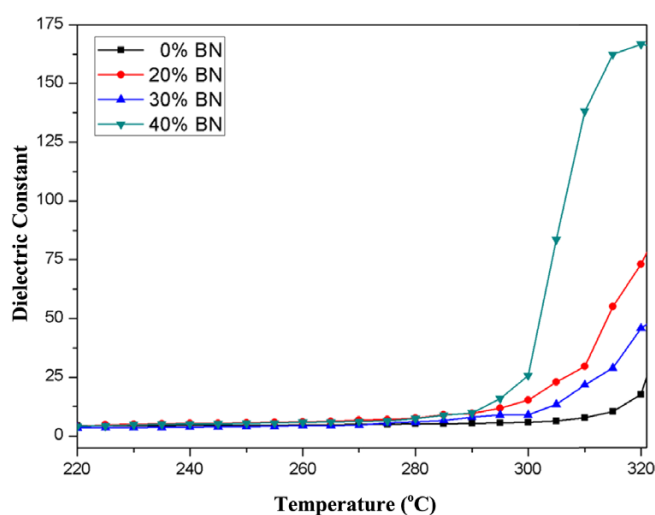


**Figure 5.** Dielectric properties with respect to temperature of CE/AG80 composites with various contents of h-BN: (a) Dielectric constant and (b) dielectric loss.

is frequency dependent parameter for the CE/AG80 matrices and decreases with increasing the frequency. It's reported that the dielectric constant would continuously decrease at high frequency due to the fact that the orientable dipolar groups and relaxation of molecular chains could not keep pace with that of the alternating field.<sup>17</sup> However, with increasing the content of h-BN fillers, the dielectric constant slightly increases. It can be assigned to the interfacial polarizations generated by the likely impurities and excess free charges associated with the suborbiculate h-BN. In Figure 4(b), low dielectric loss for the composites is presented and it's obvious that the dielectric loss is also a frequency-dependence parameter. In this case, the conduction loss and relaxation loss contribute most to the low dielectric loss for the CE/AG80/h-BN composites with respect to frequency.<sup>18</sup> In the high frequency of 20-75 kHz, an increasing of the dielectric loss for all of the composites appears that can be attributed to the significant relaxation polarization loss generated by the orientable dipoles in the molecular groups attached

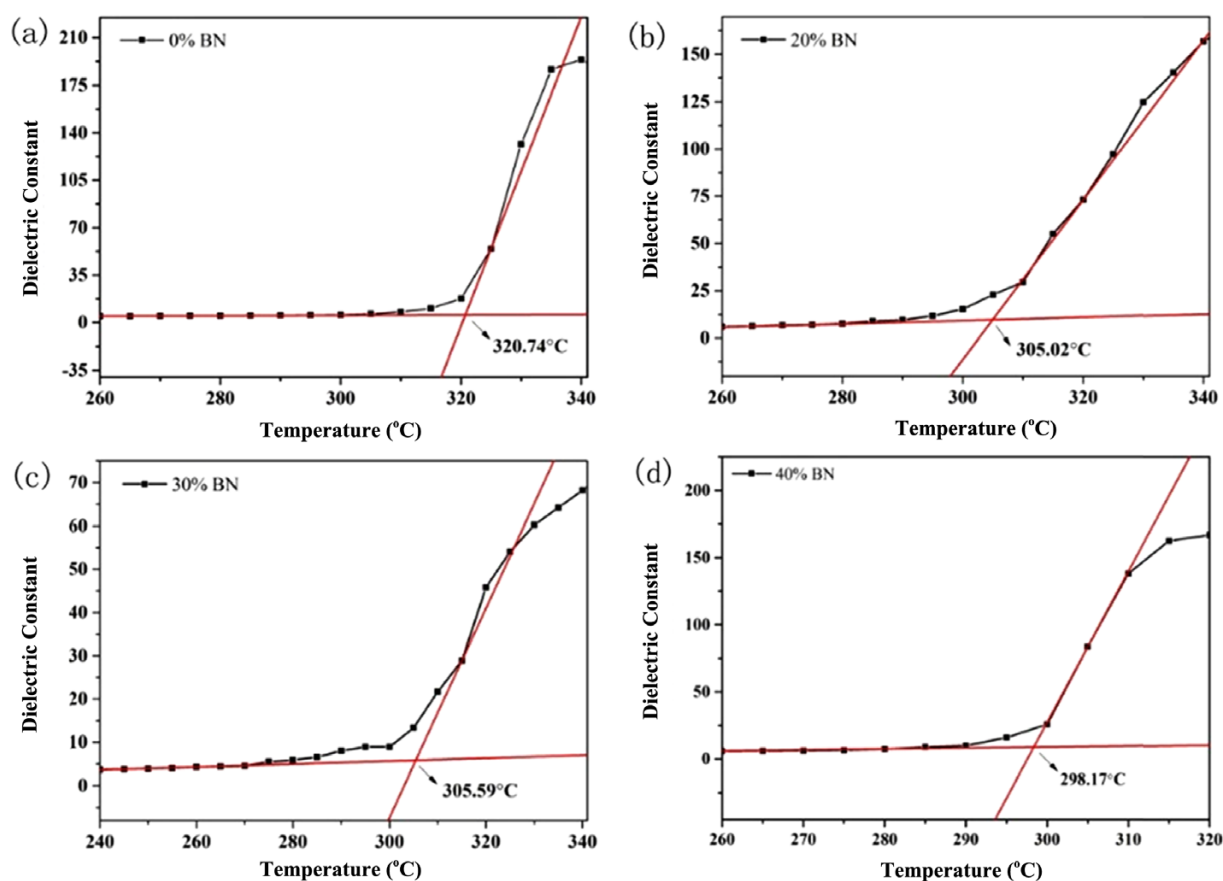


**Figure 6.** Maximum use temperatures of CE/AG80/h-BN composites with stable dielectric properties.

perpendicular to the longitudinal polymer chains.<sup>2,17</sup> Then, at the higher frequency, the conduction loss dominates the dielectric loss for the composites, showing a slight decrease.

Figure 5 shows the dielectric properties of CE/AG80/h-BN composites with respect to temperature. As discussed above, the conduction polarization and relaxation polarization coexist and combined influences on the dielectric constant and loss for the CE/AG80/h-BN composites have been observed. At low temperature, the dielectric constant is mainly assigned to the conduction polarization governed by the dipolar groups in the polymer matrices and the composites show low and stable constants.<sup>19</sup> With increasing temperature, the relaxation polarization becomes evident and affects the dielectric constant and loss significantly at about 280 °C, shown in Figure 5. It's proposed that the mutations at about 280 °C occur for the dielectric constant can be attributed to the violent mobility of polymer chains, which can be assigned to the glass transition processes.

In order to ensure that the CE/AG80/h-BN composites could be stably applied to the related fields, the maximum temperatures ( $T_{max}$ ) which the composites could be used with stable

dielectric properties are discussed. In Figure 6, we have made the tangents to the smooth stage and the rising stage of the dielectric temperature curve of the composites. The intersection point of two tangents is defined as the maximum temperatures ( $T_{max}$ ), which were collected in Table 1. It can be seen that during the temperatures below  $T_{max}$ , all of the composites present stable and low dielectric constants, which can be ascribed to the fact that the conduction polarization plays the dominant role under such a condition. As is well known, mobility of the molecular chains would significantly alter the dielectric properties including dielectric constant and loss by altering the conduction channels. Thus, in this system, the saltation of the dielectric constants can be ascribed to the mobility of polymer chains with increasing the test temperatures, that is, the  $T_{max}$  can be concluded as the glass transition temperature of the composites. In sum, the CE/AG80/h-BN composites demonstrate the stable and favorable dielectric properties with respect to frequency and temperature below their glass transition temperatures and the  $T_{max}$  of the composites is confirmed to be up to 300 °C.

**Table 1.** Saltation temperatures of the dielectric properties for CE/AG80 composites with various contents of h-BN

Samples	$T_{max}$ (°C)	$T_g$ (°C)	Dielectric constant	Dielectric loss
0 wt% h-BN	320.74	292.08	5.23	2.33
20 wt% h-BN	305.02	222.87	10.12	1.29
30 wt% h-BN	305.59	239.83	5.84	1.62
40 wt% h-BN	298.17	274.64	8.91	2.07

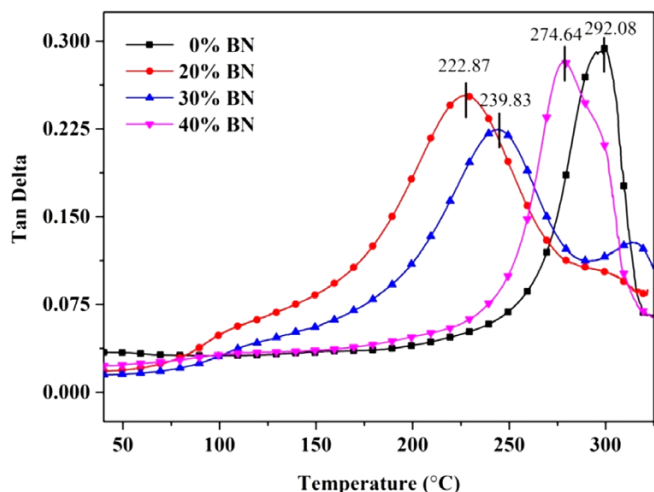


Figure 7. Tan delta of AG80/CE composites with various content of h-BN.

To further study the glass transition temperatures ( $T_g$ ) of the composite with various content of h-BN, the Tan delta is measured by DMA analysis and the temperature of its peak point is defined as the  $T_g$ . In Figure 7, all of the  $T_g$  can be observed obviously and the detailed data are collected in Table 1. It can be seen that the  $T_g$  decreases with the introduction of h-BN and the increases with increasing the content of the h-BN. It can be attributed to several reasons: first, the introduction of h-BN have affected the crosslinking degree to some extent as mentioned above, which would result to a kind of loose three dimensional network; second, the special interfacial interaction between h-BN and the resin matrix, which included a high constant or the higher mobility for the interfacial healing processes and can be attributed to the  $\pi$ -stacking noncovalent interactions in this system. Thus, the composites of CE/AG80/h-BN with 20 wt% h-BN present the lowest  $T_g$  with the effects of the aforementioned factors.

Moreover, the glass transition temperatures obtained from the results of DMA are lower than that obtained from dielectric-temperature curves. It can be attributed to the differences in the testing process. In the testing of DMA, material samples are tested though three point bending and the midpoint of sample have to be subjected to the extra down force, which would accelerate the deformation of the composites. However, in the testing of dielectric-temperature characteristics, the samples would not bear extra force. Further, the heat rate (3 °C/min) of DMA is slower than that of the dielectric-temperature testing (5 °C/min). Thus, the results of the dielectric-temperature testing are in good agreement with that of the DMA results, indicating the  $T_g$  and the maximum temperatures ( $T_{max}$ ) which

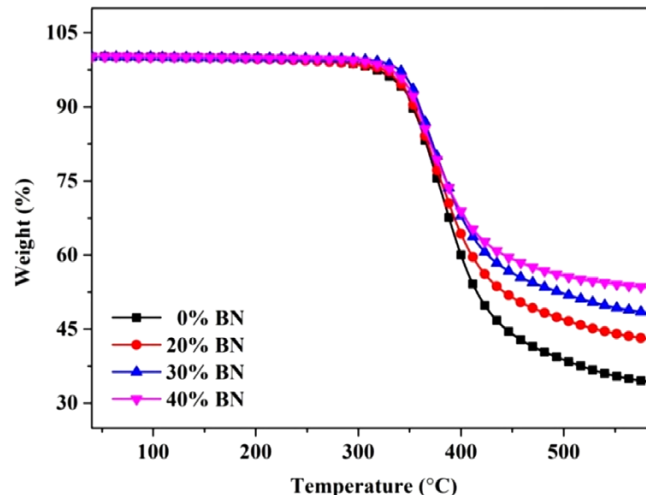


Figure 8. TGA curves of the CE/AG80/h-BN composites with various content of h-BN.

the composites could be used with stable dielectric properties.

### 3.5. Thermal stability of the CE/AG80/h-BN composites

TGA was applied to investigate the thermal stability of the CE/AG80/h-BN composites with various content of h-BN. Figure 8 showed the TGA curves of the composites and the relative data is showed in Table 2. It can be seen that all of the composites possess outstanding thermal stability with decomposition temperatures up to 330 °C. Moreover, it is observed that the decomposition temperatures of all the composites are approximate, indicating the approximate decomposition mechanism and processes. Additionally, with increasing the content of h-BN, the char yields of the composites increase, which can be ascribed to the excellent thermal stability of h-BN itself.

As is well known, the decomposition process of the composites can be described by the decomposition activate energy ( $E_a$ ), which can be obtained according to the Broido equation.<sup>20</sup> The Broido equation is showed as followed:

$$\ln \ln \left( \frac{1}{y} \right) = -(E_a/R)/T + \text{const}$$

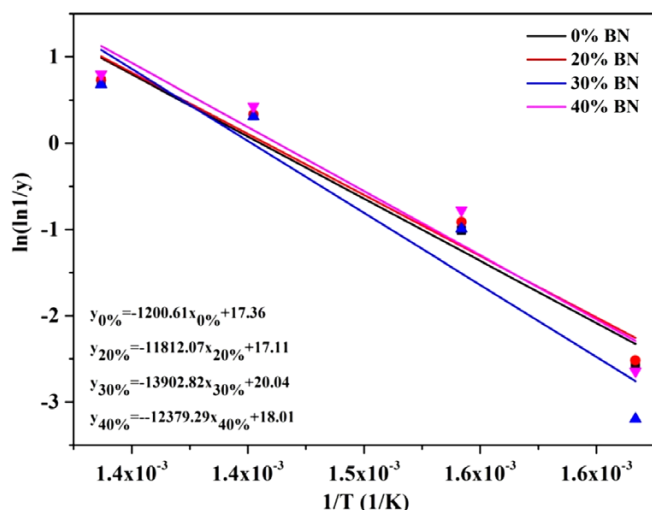
In the equation,  $y$  is the value of  $(w_t - w_\infty)/(w_0 - w_\infty)$ . Where  $w_0$ ,  $w_\infty$  and  $w_t$  are the initial weight, final weight and the weight at any temperature, respectively.  $E_a$  is the active energy and  $T$  is the temperature at  $w_t$ . The detailed data is collected in Table 2 and Table 3. The Broido plots of the composites are obtained through linear fitting (Figure 9) and the slopes of the line are calculated as the  $E_a$  which are presented in Table 3. It can be seen that all

Table 2. Detailed data of the thermal stability of the composites

Sample	$w_0$ (%)	$w_\infty$ (%)	$w_t$ (%)			
			$T_1=336.7$ °C	$T_2=370.01$ °C	$T_3=420.05$ °C	$T_4=460.01$ °C
0% BN	100	34.09	95.11	79.92	50.83	42.63
20% BN	100	42.78	95.57	81.11	56.96	50.23
30% BN	100	48.07	97.92	83.91	61.34	55.29
40% BN	100	53.2	96.78	82.73	63.3	58.29

**Table 3.** Data of the Broido equation of the composites

Sample	$w_0-w_\infty$ (%)	$w_0-w_\infty$ (%)				$E_a$ (kJ/mol)
		$T_1=336.7$ °C	$T_2=370.01$ °C	$T_3=420.05$ °C	$T_4=460.01$ °C	
0% BN	65.91	61.02	45.83	16.74	8.54	99.81
20% BN	57.22	52.79	38.33	14.18	7.45	98.21
30% BN	51.93	49.85	35.84	13.27	7.22	115.59
40% BN	46.8	43.58	29.53	10.1	5.09	102.92


**Figure 9.** The Broido curves of the composites with various content of h-BN.

of the composites show relative high  $E_a$ , indicating the relatively low decomposition rate. In sum, it can be concluded that all of the composites with various content of h-BN possess outstanding thermal stability.

#### 4. Conclusions

The CE/AG80/h-BN thermal conductive composites with low and stable dielectric properties were achieved by a simple method. It was found that the homogeneous dispersion of h-BN in the matrix could significantly maintain the low and stable dielectric constant ( $\leq 3.6$ ) and loss ( $\leq 0.01$ ) with respect to both frequency and temperature. Meanwhile, the introduction of h-BN demonstrated a remarkable enhancement of the thermal conductivity (0.54 W/mK a 1.8-fold enhancement) and significantly outperformed traditional thermal conductive fillers. Moreover, the outstanding thermal stability of the composites is confirmed by the TGA tests and the decomposition active energy obtained from Broido equation. In summary, the low and stable dielectric properties of CE/AG80/h-BN composites

with good thermal conductivity can be tuned by controlling the contents of the fillers, and it's believed that the composites should be candidates for the application of microelectronic insulation and printed circuit substrate materials.

#### References

- (1) A. Boudenne, L. Ibos, M. Fois, J. Majesté, and E. Géhin, *Compos. Part A: Appl. Sci. Manuf.*, **36**, 1545 (2005).
- (2) S. Singha and M. J. Thomas, *IEEE Trans. Dielectr. Electr. Insul.*, **15**, 12 (2008).
- (3) H. He, R. Fu, Y. Han, Y. Shen, and X. Song, *J. Mater. Sci.*, **42**, 6749 (2007).
- (4) M. J. Meziani, W. L. Song, P. Wang, F. Lu, Z. Hou, A. Anderson, H. Maimaiti, and Y. P. Sun, *Chem. Phys. Chem.*, **16**, 1339 (2015).
- (5) Z. Shi, M. Radwan, S. Kirihara, Y. Miyamoto, and Z. Jin, *Appl. Phys. Lett.*, **95**, 224104 (2009).
- (6) K. Yung and H. Liem, *J. Appl. Polym. Sci.*, **106**, 3587 (2007).
- (7) W. Zhou, C. Wang, T. Ai, K. Wu, F. Zhao, and H. Gu, *Compos. Part A: Appl. Sci. Manuf.*, **40**, 830 (2009).
- (8) K. Sato, H. Horibe, T. Shirai, Y. Hotta, H. Nakano, H. Nagai, K. Mitsuishi, and K. Watari, *J. Mater. Chem.*, **20**, 2749 (2010).
- (9) S. Z. Yu, P. Hing, and X. Hu, *Compos. Part A: Appl. Sci. Manuf.*, **33**, 289 (2002).
- (10) S. Kemaloglu, G. Ozkoc, and A. Aytac, *Polym. Compos.*, **31**, 1398 (2009).
- (11) X. Huang, L. Xie, P. Jiang, G. Wang, and F. Liu, *J. Phys. D: Appl. Phys.*, **42**, 245407 (2009).
- (12) S. Yu, P. Hing, and X. Hu, *Compos. Part A: Appl. Sci. Manuf.*, **33**, 289 (2002).
- (13) J. W. Gu, Y. Q. Guo, X. T. Yang, C. B. Liang, W. C. Geng, L. Tang, N. Li, and Q. Y. Zhang, *Compos. Part A: Appl. Sci. Manuf.*, **95**, 267 (2017).
- (14) A. Yu, P. Ramesh, M. E. Itkis, E. Bekyarova, and R. C. Haddon, *J. Phys. Chem. C*, **111**, 7565 (2007).
- (15) J. W. Gu, C. B. Liang, X. M. Zhao, B. Gan, H. Qiu, Y. Q. Guo, X. T. Yang, Q. Y. Zhang, and D. Y. Wang, *Compos. Sci. Technol.*, **139**, 83 (2017).
- (16) J. W. Gu, Z. Y. Lv, Y. L. Wu, Y. Q. Guo, L. D. Tian, H. Qiu, W. Z. Li, and Q. Y. Zhang, *Compos. Part A: Appl. Sci. Manuf.*, **94**, 209 (2017).
- (17) J. P. Eloundou, *Eur. Polym. J.*, **38**, 431 (2002).
- (18) Z. Pu, L. Chen, L. Tong, Y. Long, X. Huang, and X. Liu, *Mater. Lett.*, **109**, 116 (2013).
- (19) X. Huang, Z. Pu, M. Feng, L. Tong, and X. Liu, *Mater. Lett.*, **96**, 139 (2013).
- (20) A. Broido, *Polym. Phys.*, **2**, 1761 (1969).